Chapter 9

Basic Phytochrome B Calculations

Robert W. Smith and Christian Fleck

Abstract

Mathematical models are important tools in helping us to understand complex biological systems. Models of phytochrome-regulated systems in *Arabidopsis thaliana* have shown the importance of dimerization, nuclear transport, and thermal/dark reversion in mediating phytochrome activity and plant development. Here we go through the steps required to calculate the steady-state amounts of phytochrome subspecies relative to the total phytochrome molecule population. Starting from a simplified two-state system we expand and apply the technique to the extended phytochrome dimer model. Additionally, we provide a Python package that can automatically calculate the proportion of phytochrome B in a particular state given specific experimental conditions.

Key words Mathematical modeling, Ordinary differential equations, Phytochromes, Computer programming

1 Introduction

Plant phytochromes switch between two states (inactive P_r and active P_{fr}) in a light-dependent manner to regulate plant physiology. Phytochromes are synthesized in the P_r state within the cytosol of plant cells [1–3]. Upon exposure to red light, the phytochromes switch from P_r to P_{fr}, enter the nuclei of cells whereby they interact with a range of other proteins, form nuclear speckles/bodies, and regulate transcription [4–8]. When exposed to far-red light, the active P_{fr} conformers are switched back to the P_r state and the system is reset. As well as the light-regulated reactions, P_{fr} molecules are also constantly relaxing back to the P_r state through thermal reversion [9–12]. However, given that this process is slow, it is often only important for regulating phytochrome dynamics in darkness or under low intensity light [12, 13]. The reactions shown in Fig. 1a form the basic two-state phytochrome system [3, 13, 14].

In the presence of synthesis and degradation reactions, experimentally measuring the proportions of phytochrome populations within specific states, and how fast they conformationally

Andreas Hiltbrunner (ed.), *Phytochromes: Methods and Protocols*, Methods in Molecular Biology, vol. 2026, https://doi.org/10.1007/978-1-4939-9612-4_9,

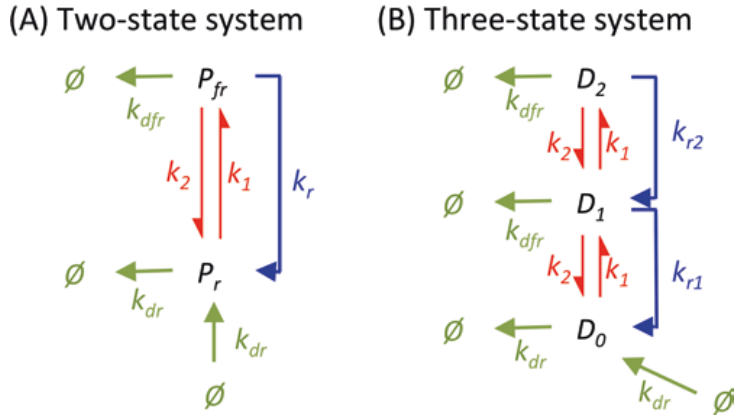

Fig. 1 Phytochrome B dynamics in plants. Simplified schematic representations of phytochrome B dynamics in plants. (**a**) The two-state system whereby phyB switches between P_r and P_{fr} states. (**b**) The three-state system whereby dimers of phyB P_r and P_{fr} are formed. Here, $D_0 = P_r - P_r$, $D_1 = P_r - P_{fr}$, and $D_2 = P_{fr} - P_{fr}$ dimers. Parameters: k_1, k_2=light-regulated photoconversion rates; k_{di} = degradation rates; k_{ri} = thermal reversion rate of P_{fr} to P_r state. Light-regulated reactions are colored red, thermal reversion in blue, and degradation or synthesis reactions in green

change from one state to another, is often difficult. Consequently, mathematical models and computational optimization techniques have been utilized to provide a better understanding as to how phytochrome subpopulations regulate plant development [3, 13, 15–17]. These models have helped explain how phytochrome B (phyB) dynamics relate to hypocotyl elongation of *Arabidopsis thaliana* and why phytochrome A shows activity under far-red light [3, 12, 14].

To highlight the utility of mathematical models, the two-state system of phyB was constructed mathematically and matched to data showing thermal reversion of P_{fr}, degradation kinetics, nuclei speckle formation, and, ultimately, hypocotyl elongation all under a range of different light conditions (Fig. 1a; [3]). However, this model was unable to explain why hypocotyl elongation is not strongly inhibited under high intensity ~700 nm light [12]. The two-state model was extended to incorporate phyB dimerization—a phenomenon that had been previously observed experimentally [18]. The resulting three-state model (P_r–P_r, P_r–P_{fr} and P_{fr}–P_{fr} dimers rather than P_r and P_{fr} molecules in the two-state model) correctly matched fluence-response curves of hypocotyl elongation under high intensity 690–716 nm light (Fig. 1b; [12]).

Here, we discuss the two-state and three-state models, showing that the steady-state (after prolonged periods of light exposure) proportions of phytochrome species can be directly calculated given the experimental conditions. We then introduce a Python script that automatically performs these calculations that we hope the photobiology community will find of use in the future.

2 Methods

2.1 Models

2.1.1 Original Models and Simplifying Assumptions

Both of the original models proposed by Rausenberger et al. and Klose et al. are too complex to be analyzed at steady state without numerical simulations [3, 12]. Here, we shall quickly review the two systems and the simplifying assumptions we have made to aid the analytical calculations introduced in the following sections. We refer readers to the original publications for further details and model equations.

As well as photoconversion between different phyB states, the two models also include a range of other biological processes (Fig. 2): intracellular transport from cytoplasm to nucleus (defined by parameter k_{in} in Fig. 2) and, ultimately, into nuclear bodies (denoted 'NB' in Fig. 2, where k_3 and k_4 are the P_{fr}-dependent NB association and dissociation rates, and k_5 is the P_r-dependent NB dissociation rate [12]). Within each compartment, the degrada-

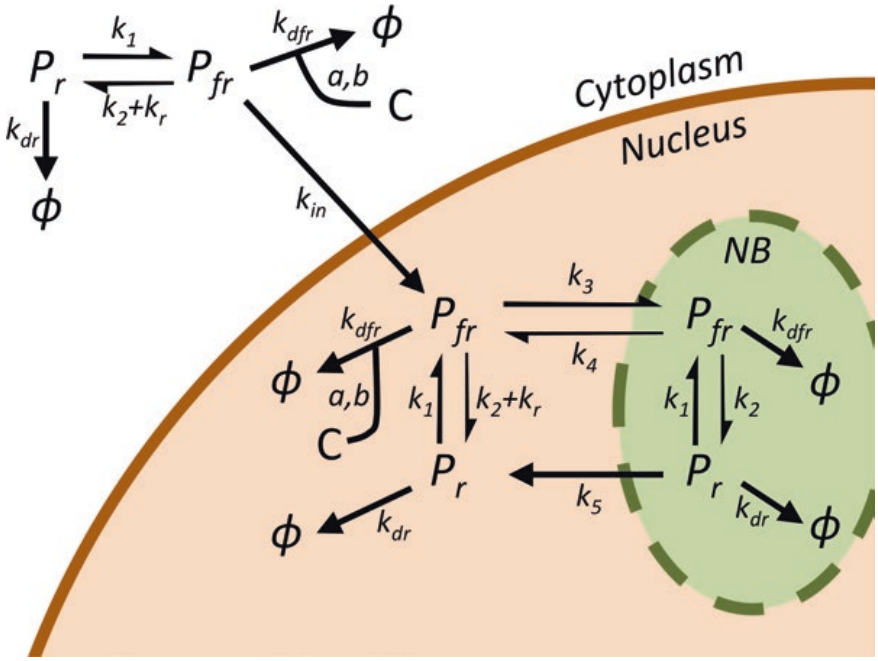

Fig. 2 Phytochrome B dynamics captured in full models. Schematic of all the biological processes in the full models of phyB dynamics [3, 12]. As in Fig. 1, phyB undergoes photoconversion, thermal reversion and degradation. However, in the full models, phyB is also transported between cellular compartments, including the cytoplasm, nucleus, and nuclear speckles/bodies (NB). Within the NBs there is no thermal reversion process. Degradation processes also depend on compartment, whereby an interacting protein, C, enhances P_{fr} degradation in the cytoplasm and nucleus. The parameter k_{in} represents nuclear import of phyB, k_3 and k_4 are the P_{fr}-dependent NB association and dissociation rates, k_5 is the P_r-dependent NB dissociation rate, and a and b are indicative of the sensitivity of P_{fr} to C and the enhancement of degradation by C, respectively

tion and thermal reversion of phyB differs. As observed experimentally, thermal reversion is strongly suppressed within NBs due to their prolonged visibility after long periods of darkness [3]. Degradation rates of P_r and P_{fr} also differ due to the experimental observation that phyB degrades faster under red light when compared to levels of phyB in etiolated seedlings [3]. This suggests that P_{fr} degrades faster than P_r. Further iterations of the model went on to include compartment-dependent degradation mechanisms of P_{fr} whereby degradation is enhanced by phyB-interacting proteins in the cytoplasm and nucleus but not in NBs [12]. These degradation mechanisms are controlled by two parameters (a and b in Fig. 2 and Table 1) that determine the affinity between P_{fr} and an interacting protein (a) and the enhancement of degradation due to the interaction (b).

Whilst these models, when simulated numerically, are more accurate at describing phyB dynamics, they are intractable to obtain analytic *estimates* of species concentrations in the phyB system. In order to perform the analytical derivations below we make two simplifying assumptions. First, P_r, P_{fr}, and their respective dimers degrade at the same rate in *all* cellular compartments. Second, we

Table 1
Format for input file detailing simulated parameter values

Parameter	Biological interpretation	Units	Value 1 (default values)	⋯	Value X (simulating no dark reversion)
k_{dr}	Phytochrome degradation	min^{-1}	0.00061	⋯	0.00061
k_{dfr}	P_{fr}-specific degradation	min^{-1}	49.57	⋯	49.57
k_{r1}	D_1 dark reversion	min^{-1}	0.497	⋯	0
k_{r2}	D_2 dark reversion	min^{-1}	0.0051	⋯	0
k_{31}	D_1 NB formation	min^{-1}	1.36	⋯	1.36
k_{32}	D_2 NB formation	min^{-1}	4.43	⋯	4.43
k_{41}	D_1 NB breakdown	min^{-1}	4.1	⋯	4.1
k_{42}	D_2 NB breakdown	min^{-1}	0.13	⋯	0.13
k_5	D_0 NB breakdown	min^{-1}	0.03	⋯	0.03
k_{in}	P_{fr} nuclear import	min^{-1}	58.4	⋯	58.4
M	Number of NBs	–	6	⋯	6
a	Sensitivity of P_{fr}-specific degradation	–	0.56	⋯	0.56
b	Strength of P_{fr}-specific degradation	–	9	⋯	9

Up to X different parameter sets can be simulated. *See* Fig. 2 for a schematic illustration of parameters biological interpretation. The first numeric column shows the default values. See text for details about parameter notation

allow for thermal reversion within NBs. These two assumptions (although biologically inaccurate) allow us to ignore cellular compartments in our model and construct simpler, mathematically tractable systems with which to estimate the proportions of P_r, P_{fr}, D_0, D_1, and D_2 within cells.

2.1.2 Two-State Model

The two-state model incorporates dynamics for the P_r and P_{fr} concentrations within a cell. The ordinary differential equations (ODEs) read as follows:

$$\begin{aligned}\frac{dP_r}{dt} &= k_{dr}\left(1-P_r\right)+\left(k_2+k_r\right)P_{fr}-k_1P_r\\ \frac{dP_{fr}}{dt} &= k_1P_r-\left(k_2+k_r+k_{dfr}\right)P_{fr},\end{aligned} \tag{1}$$

where dx/dt is the change in concentration x over a time-step dt, k_r, is the thermal reversion rate, k_{dr} and k_{dfr} are the conformation-dependent degradation rates, and k_1 and k_2 are the light-regulated photoconversion rates. We normalized the equations such that the amount of P_r before light exposure is equal to 1, that is, 100% of the phyB population is in the P_r state. The light-regulated photoconversion rates are given by $k_i = \sum_{\lambda} N_\lambda \sigma_i^\lambda$, where N_λ is the wavelength-dependent light intensity of the experimental conditions in μmol/m²s and σ^λ is the photoconversion cross-section at wavelength λ between the two states in m²/mol (*see* **Note 1**; [13]).

2.1.3 Three-State Model

Similarly to the two-state model, we can simplify the model proposed by Klose et al. to read as follows:

$$\begin{aligned}\frac{dD_0}{dt} &= k_{dr}\left(1-D_0\right)+\left(k_2+k_{r1}\right)D_1-2k_1D_0\\ \frac{dD_1}{dt} &= 2k_1D_0+2\left(k_2+k_{r2}\right)D_2-\left(k_1+k_2+k_{r1}+k_{dfr}\right)D_1\\ \frac{dD_2}{dt} &= k_1D_1-\left[2\left(k_2+k_{r2}\right)+k_{dfr}\right]D_2\end{aligned} \tag{2}$$

The states of the dimer are denoted by $D_0 = P_r - P_r$, $D_1 = P_r - P_{fr}$ and $D_2 = P_{fr} - P_{fr}$ [12]. The thermal reversion of D_2 is slower than D_1 such that $k_{r2} < k_{r1}$. Again the model is normalized such that the amount of D_0 before light exposure is equal to 1. Note that, in this model, the multiplication of conformation switching from the homodimers to the heterodimer by 2 represents the fact that the heterodimer can take two different heterodimer forms, $P_r - P_{fr}$ and $P_{fr} - P_r$, such that D_1 is the total concentration of these two forms.

2.2 Steady-State Analysis

Here we will go through the steps required to estimate the proportion of the phyB molecular population in a given state after prolonged experimental conditions. To do this we assume that the system has reached steady state.

2.2.1 Definition: Steady State

When we refer to solving a mathematical model at *steady state* what we are implying is that the concentration of each system component does not change over time, that is, they are constant. Thus, all equations of the system can be set $\mathrm{d}x/\mathrm{d}t = 0$. In relation to the phytochrome system this means that the sample has been exposed to a given light condition for a long enough period of time that the concentrations of P_r, P_{fr}, and their respective dimers are stable.

2.2.2 Two-State Model

By setting $\mathrm{d}P_{fr}/\mathrm{d}t = 0$ in Eq. 1, we get

$$k_1 P_r - \left(k_2 + k_r + k_{dfr}\right) P_{fr} = 0.$$

From this, it is clear to see that

$$k_1 \left(P_r + P_{fr}\right) - \left(k_1 + k_2 + k_r + k_{dfr}\right) P_{fr} = 0,$$

is also true as the added $k_1 P_{fr}$ terms cancel with each other.

Thus, using $P_{tot} = P_r + P_{fr}$, rearrangement leads to

$$\begin{aligned} \frac{P_{fr}}{P_{tot}} &= \frac{k_1}{k_1 + k_2 + k_r + k_{dfr}} \\ \frac{P_r}{P_{tot}} &= 1 - \frac{P_{fr}}{P_{tot}} = \frac{k_2 + k_r + k_{dfr}}{k_1 + k_2 + k_r + k_{dfr}}. \end{aligned} \tag{3}$$

Using these expressions, we can also go one step further and ask what the effect of light intensity is on the system. By substituting $k_i = \sum_\lambda N_\lambda \sigma_i^\lambda$ into the above expressions we get

$$\frac{P_{fr}}{P_{tot}} = \frac{\sum_\lambda N_\lambda \sigma_r^\lambda}{\sum_\lambda N_\lambda \left(\sigma_r^\lambda + \sigma_{fr}^\lambda\right) + k_r + k_{dfr}}. \tag{4}$$

From this, as $N_\lambda \to \infty$, the effects of dark reversion and degradation of P_{fr} become negligible compared to the photoconversion reactions. Hence, the proportion of P_{fr} in the system within this limit is dominated by the photoconversion spectra or light-regulated reactions

$$\lim_{N_\lambda \to \infty} \frac{P_{fr}}{P_{tot}} = \frac{\sum_\lambda N_\lambda \sigma_r^\lambda}{\sum_\lambda N_\lambda \left(\sigma_r^\lambda + \sigma_{fr}^\lambda\right)}. \tag{5}$$

2.2.3 Three-State Model

In order to obtain expressions for D_0, D_1, D_2, and P_{fr}/P_{tot} from the three-state model, we need to simplify the system. We do this in two ways. First, we reduce the system from three variables to two by using $D_{tot} = D_0 + D_1 + D_2$, such that $D_0 = D_{tot} - D_1 - D_2$. This means that we go from having three equations and three unknown variables to having three equations and two unknowns (D_1/D_{tot} and D_2/D_{tot}). Second, we set $k_{dr} = 0$, implying that synthesis or degradation of phyB D_0 is very slow relative to other reactions in

the system [3]. This removes the constant term from the equation for dD_0/dt and allows the system to be rewritten into new variables. Thus, upon setting the time derivatives to zero we can rewrite the system as

$$\begin{aligned}
0 &= \left(2k_1 + k_2 + k_{r1}\right)\frac{D_1}{D_{tot}} - 2k_1\left(1 - \frac{D_2}{D_{tot}}\right) \\
0 &= 2k_1 + 2\left(k_2 + k_{r2} - k_1\right)\frac{D_2}{D_{tot}} - \left(3k_1 + k_2 + k_{r1} + k_{dfr}\right)\frac{D_1}{D_{tot}} \\
0 &= k_1\frac{D_1}{D_{tot}} - \left[2\left(k_2 + k_{r2}\right) + k_{dfr}\right]\frac{D_2}{D_{tot}},
\end{aligned} \tag{6}$$

Substituting the third expression of Eq. 6 into the first to remove the D_1/D_{tot} terms yields the following:

$$\begin{aligned}
0 &= \left(2k_1 + k_2 + k_{r1}\right)\frac{2\left(k_2 + k_{r2}\right) + k_{dfr}}{k_1}\frac{D_2}{D_{tot}} + 2k_1\left(1 - \frac{D_2}{D_{tot}}\right) \\
\frac{D_2}{D_{tot}} &= \frac{2k_1^2}{2k_1^2 + \left(2k_1 + k_2 + k_{r1}\right)\left[2\left(k_2 + k_{r2}\right) + k_{dfr}\right]}
\end{aligned} \tag{7}$$

Further substitution of this term into the second expression of Eq. 6 and solving for D_1/D_{tot} gives

$$\begin{aligned}
\frac{D_1}{D_{tot}} &= \frac{1}{3k_1 + k_2 + k_{r1} + k_{dfr}}\left[2k_1 + \frac{4k_1^2\left(k_2 + k_{r2} - k_1\right)}{2k_1^2 + \left(2k_1 + k_2 + k_{r1}\right)\left[2\left(k_2 + k_{r2}\right) + k_{dfr}\right]}\right] \\
&= \frac{2k_1\left\{2k_1^2 + \left(2k_1 + k_2 + k_{r1}\right)\left[2\left(k_2 + k_{r2}\right) + k_{dfr}\right]\right\} + 4k_1^2\left(k_2 + k_{r2} - k_1\right)}{\left(3k_1 + k_2 + k_{r1} + k_{dfr}\right)\left\{2k_1^2 + \left(2k_1 + k_2 + k_{r1}\right)\left[2\left(k_2 + k_{r2}\right) + k_{dfr}\right]\right\}}.
\end{aligned} \tag{8}$$

Finally, using the fact that $D_{tot} = D_0 + D_1 + D_2$, we obtain

$$\begin{aligned}
\frac{D_0}{D_{tot}} &= 1 - \frac{D_1}{D_{tot}} - \frac{D_2}{D_{tot}} \\
&= \frac{\left(k_1 + k_2 + k_{r1} + k_{dfr}\right)\left\{2k_1^2 + \left(2k_1 + k_2 + k_{r1}\right)\left[2\left(k_2 + k_{r2}\right) + k_{dfr}\right]\right\}}{\left(3k_1 + k_2 + k_{r1} + k_{dfr}\right)\left\{2k_1^2 + \left(2k_1 + k_2 + k_{r1}\right)\left[2\left(k_2 + k_{r2}\right) + k_{dfr}\right]\right\}} \\
&= -\frac{4k_1^2\left(k_2 + k_{r2} - k_1\right) + 2k_1^2}{\left(3k_1 + k_2 + k_{r1} + k_{dfr}\right)\left\{2k_1^2 + \left(2k_1 + k_2 + k_{r1}\right)\left[2\left(k_2 + k_{r2}\right) + k_{dfr}\right]\right\}}.
\end{aligned} \tag{9}$$

We can now use these expressions to calculate the total amount of P_r and P_{fr} in the system at steady state. Recall that in D_2 we have all the phyB molecules in the P_{fr} state, whilst in D_1 half the molecules are in the P_{fr} state. This means that

$$\frac{P_{\mathrm{fr}}}{P_{\mathrm{tot}}} = \frac{D_2 + D_1/2}{D_{\mathrm{tot}}} \tag{10}$$

and

$$\frac{P_{\mathrm{r}}}{P_{\mathrm{tot}}} = 1 - \frac{P_{\mathrm{fr}}}{P_{\mathrm{tot}}} = \frac{D_0 + D_1/2}{D_{\mathrm{tot}}}. \tag{11}$$

We shall not provide the exact expressions here, but one should note that as $N_\lambda \to \infty$ (or equivalently $\{k_{\mathrm{r1}}, k_{\mathrm{r2}}, k_{\mathrm{dfr}}\} \to 0$) the resulting pool size of P_{fr} is given by

$$\lim_{N_\lambda \to \infty} \frac{P_{\mathrm{fr}}}{P_{\mathrm{tot}}} = \frac{\sum_\lambda N_\lambda \sigma_{\mathrm{r}}^\lambda}{\sum_\lambda N_\lambda \left(\sigma_{\mathrm{r}}^\lambda + \sigma_{\mathrm{fr}}^\lambda\right)}.$$

as is the case for the simpler two-state model in Eq. 5.

2.3 Computational Tool

We hope, from the above derivations, that we have shown how the mathematical models of phytochrome activity can be analyzed to estimate the steady-state percentage of P_{fr} in the system. To aid the photobiology community, we have developed a computational tool that numerically simulates the full model proposed by Klose et al. [12] or analytically solves the simplified three-state model given a set of input conditions. In Fig. 3, we provide a workflow as to how the algorithm functions and what the output could look like. These input conditions can be formatted within text files or can be submitted to the tool from the command-line interface. The calculator can be downloaded from http://gitlab.com/

Fig. 3 Overview of computational tool. Schematic overview of the computational tool. Given the input answers to specific questions (*see* Subheading 2.3) the Python script simulates levels of phytochrome system components. The output is in tabular form, providing the values for each experimental condition requested

wurssb/Phytochrome_Calculator (*see* **Note 2**). Examples of input files required to use the calculator can also be found here. To calculate the relevant values the following questions need to be answered.

2.3.1 Would You Like to Change Any Kinetic Rates Within the phyB System?

The amount of P_{fr} within the phytochrome system depends on the rates at which phyB switches between different states, thermal reversion and degradation (Eqs. 4 and 10). Consequently, users can either use the published values of the degradation and thermal reversion rates (as default) or change them to any value they desire. This could be advantageous if, for example, one wished to know how much P_{fr} exists in a molecule population of mutated phyB whereby the thermal reversion rate (given by the k_{r*} parameters in Figs. 1 and 2 and Table 1) is altered, as in [10, 11]. The altered parameter values can be input into the calculator from the command line or using a text file containing a table similar to Table 1 where the first numerical column shows the default values published by [12].

2.3.2 Would You Like to Use the Default Photoconversion Spectra?

As discussed above, P_{fr} levels are dependent on the speed of light-regulated reactions (k_1 and k_2 above) as determined by the photoconversion spectra (σ_r^{λ} and σ_{fr}^{λ}; *see* Eqs. 4 and 10). By default, our calculator uses the values published for full-length phytochromes [13]. However, one may wish to alter the light-regulated photoconversion rates in the phyB system or measure new photoconversion spectra. For example, the N-terminal 650 amino acid truncated form of the phyB protein used in synthetic biology has recently been shown to respond to light more slowly in vitro than the full-length protein in vivo [16]. Thus, if a user had measured or knew that a particular phyB variant had altered photoconversion spectra compared to the full-length protein, then the user can calculate P_{fr} levels with these new values. The measured photoconversion spectra should be stored in a text file following the table structure shown in Table 2.

Table 2
Format for input file allowing multiple photoconversion spectra to be simulated

Wavelength, λ (nm)	σ_r^1 **(μmol/m²s)**	σ_{fr}^1 **(μmol/m²s)**	σ_r^2 **(μmol/m²s)**	σ_{fr}^2 **(μmol/m²s)**	⋯	σ_r^X **(μmol/m²s)**	σ_{fr}^X **(μmol/m²s)**
300	1404.0	728.3	67.12	71.52	⋯	4.953	0.468
310	906.1	572.7	79.26	67.39	⋯	5.798	0.352
320	677.7	481.0	101.0	64.71	⋯	6.957	0.468
⋮	⋮	⋮	⋮	⋮	⋱	⋮	⋮

Up to *X* different photoconversion spectra can be simulated. See text for details about parameter notation

Table 3
Format for input file containing experimental conditions

λ_1	N_{λ_1}	λ_2	N_{λ_2}	⋯	λ_X	N_{λ_X}
640	0.0834	665	5.0	⋯	740	1.0
641	0.0824			⋯		
642	0.0829			⋯		
⋮	⋮	⋮	⋮	⋱	⋮	⋮

Up to X experimental conditions can be simulated, including light distributions. Here λ_i is the wavelength of the light source (either a single value or a distribution) and N_{λ_i} is the corresponding light intensity

2.3.3 Do You Have an Input File of Measured Light Intensities?

In order to calculate the amount of P_{fr}, one needs to specify the experimental conditions that determine k_1 and k_2. Users must provide a wavelength (or wavelengths) and their respective light intensities at which to calculate steady-state P_{fr} levels. Importantly, users can either calculate these values at a single wavelength with a single intensity (as would be the case if one would use idealized lasers experimentally), across a distribution of wavelengths (as is the case when using LEDs experimentally) or across a complete light spectrum (as is the case when measuring, for example, natural sunlight). The measured light spectrum can be input into the calculator from the screen or with a text file using the table format shown in Table 3. This provides users with the freedom to simulate any experimental condition currently found in the published literature.

2.3.4 Would You Like to Solve the System Analytically or Numerically?

In the above derivations, we have shown how the full dynamic system of phyB activity can be reduced under steady-state conditions using simplifying assumptions to a single equation determining the percentage of P_{fr} in the molecule population. Here we allow the users to choose whether they wish to calculate the percentage of P_{fr} using the analytical steady-state equations or the full dynamic system schematically illustrated in Fig. 2 [3, 12]. In **Note 3** we discuss the conditions under which the two solutions differ.

2.3.5 Enter Path for Results File

Finally, we require the user to specify where they would like their results to be saved. The results are printed to the screen and a text file is automatically created containing different amounts of information depending on whether the system has been simulated numerically or analytically. If the system has been simulated numerically then information with regards to the relative levels of each dimer form, the total amount of P_{r} and P_{fr} in the system, how much P_{fr} is in the nucleus, how much D_2 is in the nucleus, and how much phyB is in nuclear speckles can be obtained. However, if the system is simulated analytically then one can only obtain informa-

Table 4
Format of output file

Simulation	Total D_0	Total D_1	Total D_2	Total P_r	Total P_{fr}	Total nuclear P_{fr}	Total nuclear D_2	Total phy in NBs
Analytic	0.98	0.02	0.00	0.99	0.01	–	–	–
Numeric	0.98	0.02	0.00	0.99	0.01	0.01	0.00	0.17

Example of which information is contained in the output file given that the phytochrome system is simulated either analytically or numerically

tion about the relative levels of each dimer form, the total amount of P_r and P_{fr} in the system since the analytic calculation does not take into account different cellular compartments (*see* Subheading 2.2.2 above). From the current published literature, this information should be sufficient to relate phyB activity to physiological responses such as hypocotyl elongation [12]. The output file is organized to provide this information in tabular form (as seen in Table 4) for all the requested sets of kinetic rates, photoconversion spectra, and experimental conditions specified above.

3 Notes

1. An important aspect of mathematical modeling is ensuring that the equations have consistent dimensions. For example, all the k_i's in the models outlined above are in units min^{-1} such that $dx/dt = [\text{concentration}] \cdot [\text{min}]^{-1}$. However,

$$k_1 = \sum_{\lambda_{max}}^{\lambda=\lambda_{min}} N_\lambda \sigma_r^\lambda = \frac{\mu mol}{m^2 s} \times \frac{m^2}{mol} \neq \frac{1}{\text{min}}.$$

Thus, the light-regulated parameters need to be rescaled by

$$\alpha \sim \frac{mol}{\mu mol} \times \frac{s}{\text{min}} = 6 \times 10^{-5} min^{-1},$$

such that $k_1 \rightarrow \alpha k_1$. The same needs to be applied to k_2 to ensure that one calculates the correct dynamics of the phyB system and the P_{fr} levels.

In these expressions, λ_{min} and λ_{max} represent the minimum and maximum wavelengths for which the photoconversion spectra σ^λ is measured. Thus, even if light intensity is measured at other wavelengths, the k_i's can only be calculated if the photoconversion spectra are known. As default in our computational tool, we use the photoconversion spectra measured by [13] where λ_{min} = 300 nm and λ_{max} = 770 nm. Further methods have also been developed to calculate the photoconversion spectra for phytochrome proteins [16].

2. The code was written using Python version 2.7 with NumPy version 1.8 and SciPy version 0.13. We recommend users to maintain use of Python version 2.7 when running the calculator, but our current implementation should be compatible with newer versions of NumPy and SciPy. Detailed information about the tool's usage, as discussed above, can also be found in the README files and we encourage users to read these before using the program. All input files need to be generated as comma-delimited tables with the columns shown in Tables 1, 2, and 3. Example files are provided with the Python scripts.
3. Within the computational tool, we provide the user with the option of analyzing the phyB system numerically or analytically. The choice of technique used depends on what the user wishes to analyze. For example, solving the full system numerically allows the user to observe how altering speckle formation kinetics (the parameters k_{3*}, k_{4*}, or k_5 in Table 1, *see* Subheading 2.1.1) leads to changes in P_{fr}/P_{tot}. However, whilst solving the system analytically restricts the number of parameters that can be changed in the system, it does allow the user to study a wider range of experimental conditions easily. In calculating the analytical expressions, we used the steady-state assumption and simplified models (*see* Subheading 2). However, in our numerical solver, the user can define how long they wish to simulate the phyB system for. This means that, under certain conditions, the analytical and numerical solutions of the phyB system will differ. We have already shown above that when light intensity is high, the amount of P_{fr} in the system at steady state tends to the ratio of photoconversion spectra. This is similarly the case for the numerical solution. However, when light intensity is low (i.e., when $N_\lambda < 0.1$ μmol/m^{2}s), the dynamics of the phyB system are slower, meaning that the steady-state level of P_{fr} will not be reached and will require longer simulation time to simulate. Thus, the numerical solution after short time-periods shall not match the steady-state level under these conditions. Users are advised to take this into consideration when performing their analyses.

Acknowledgments

We would like to thank Andreas Hiltbrunner and Rik van Rosmalen for testing the tool and for providing valuable feedback as to its usage and how it can be made easier for users. RWS is funded by FP7 Marie Curie Initial Training Network grant agreement number

316723 and EU Horizon 2020 grant agreement number 634942. CF is funded by HFSP Research grant RGP0025/2013.

References

1. Rüdiger W, Thümmler F, Cmiel E et al (1983) Chromophore structure of the physiologically active form (Pfr) of phytochrome. Proc Natl Acad Sci U S A 80:6244–6248
2. Li L, Lagarias JC (1992) Phytochrome assembly. J Biol Chem 267:19204–19210
3. Rausenberger J, Hussong A, Kircher S et al (2010) An integrative model for phytochrome B mediated photomorphogenesis: from protein dynamics to physiology. PLoS One 5:e10721
4. Chen M, Schwab R, Chory J (2003) Characterization of the requirements for localization of phytochrome B to nuclear bodies. Proc Natl Acad Sci U S A 100:14493–14498
5. Tepperman JM, Hudson ME, Khanna R et al (2004) Expression profiling of phyB mutant demonstrates substantial contribution of other phytochromes to red-light-regulated gene expression during seedling de-etiolation. Plant J 38:725–739
6. Al-Sady B, Kikis EA, Monte E et al (2008) Mechanistic duality of transcription factor function in phytochrome signaling. Proc Natl Acad Sci U S A 105:2232–2237
7. Park E, Park J, Kim J et al (2012) Phytochrome B inhibits binding of phytochrome-interacting factors to their target promoters. Plant J 72:537–546
8. Pfeiffer A, Nagel MK, Popp C et al (2012) Interaction with plant transcription factors can mediate nuclear import of phytochrome B. Proc Natl Acad Sci U S A 109:5892–5897
9. Schäfer E, Schmidt W (1974) Temperature dependence of phytochrome dark reactions. Planta 116:257–266
10. Medzihradszky M, Bindics J, Ádám É et al (2013) Phosphorylation of phytochrome B inhibits light-induced signaling via accelerated dark reversion in Arabidopsis. Plant Cell 25:535–544
11. Burgie ES, Bussell AN, Walker JM et al (2014) Crystal structure of the photosensing module from a red/far-red light-absorbing plant phytochrome. Proc Natl Acad Sci U S A 111:10179–10184
12. Klose C, Venezia F, Hussong A et al (2015) Systematic analysis of how phytochrome B dimerization determines its specificity. Nat Plants 1:15090
13. Mancinelli AL (1994) The physiology of phytochrome action. In: Kendrick RE, Kronenberg GMH (eds) Photomorphogenesis in plants. Kluwer Academic Publishers, Dordrecht
14. Rausenberger J, Tscheuschler A, Nordmeier W et al (2011) Photoconversion and nuclear trafficking cycles determine phytochrome A's response profile to far-red light. Cell 146:813–825
15. Hennig L, Büche C, Schäfer E (2000) Degradation of phytochrome A and the high irradiance response in Arabidopsis: a kinetic analysis. Plant Cell Environ 23:727–734
16. Smith RW, Helwig B, Westphal AH et al (2016) Unearthing the transition rates between photoreceptor conformers. BMC Syst Biol 10:110
17. Smith RW, Helwig B, Westphal AH et al (2017) Interactions between phyB and PIF proteins alter thermal reversion reactions in vitro. Photochem Photobiol 93:1525–1531
18. Li H, Zhang J, Vierstra RD et al (2010) Quaternary organization of a phytochrome dimer as revealed by cryoelectron microscopy. Proc Natl Acad Sci U S A 107:10872–10877